Electronic Supplementary Material (ESI) for Sustainable Energy & Fuels.

Supplementary Information

A flexible graphene-carbon fiber composite electrode with high surface area-normalized capacitance

Xiaoming Sun, Hao Lu, Thomas E. Rufford, Rohit Ranganathan Gaddam, Timothy T. Duignan, Xin Fan, X. S. Zhao*

School of Chemical Engineering, The University of Queensland, St Lucia, Brisbane, QLD 4072, Australia.

*E-mail: *george.zhao@uq.edu.au*

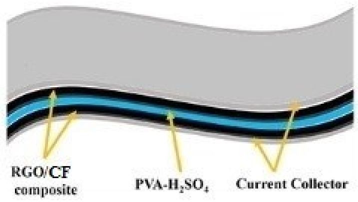

Fig. S1 Schematic illustration of the all solid -state supercapacitors.

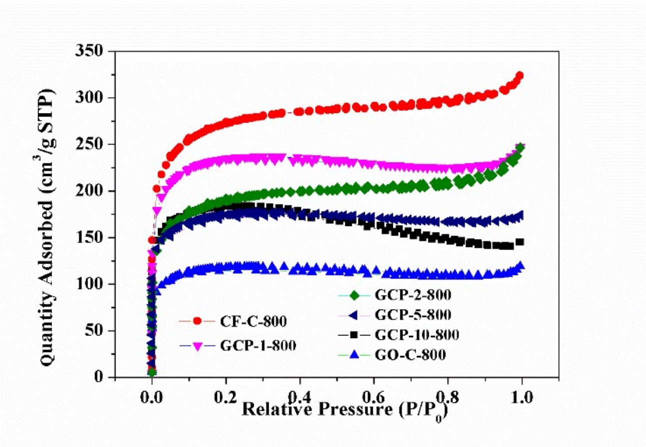

Fig. S2 N_2 adsorption/desorption isotherms of GO-C-800, CP-C-800, GCP-1-800, GCP-2-800, GCP-5-800, and GCP-10-800.

Table S1 Raman intensity ratio I_D/I_G of various samples

Sample	I_D/I_G
CP-C-800	0.94
GCP-1-800	0.92
GCP-2-800	0.91
GCP-5-800	0.86
GCP-10-800	0.85
GO-C-800	0.82

We can provide an upper estimate for the optimal GO loading by determining at what point the total surface area of added GO will exceed the total available surface area of CP that it can adsorb to. At this point we can expect the benefits of adding GO to be negligible as any additional GO will simply aggregate. This point can be estimated by taking the total mass per unit area of CP (1.8 mg cm^{-2}), multiply by its SSA (670 m^2 g^{-1}) to give an effective SSA of 1.21 m^2 cm^{-2} and then divide by the SSA of graphene (2630 m^2 g^{-1}) to determine a maximum optimal loading of 0.46 mg cm^{-2}.

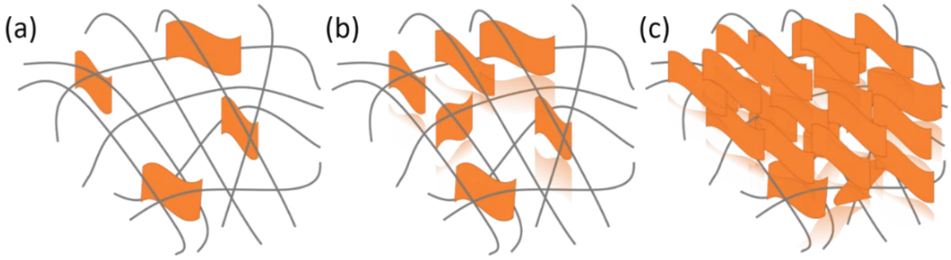

Fig. S3 Illustration scheme for different GO loading with CF (a) low content, (b) optimized content, and (c) high content.

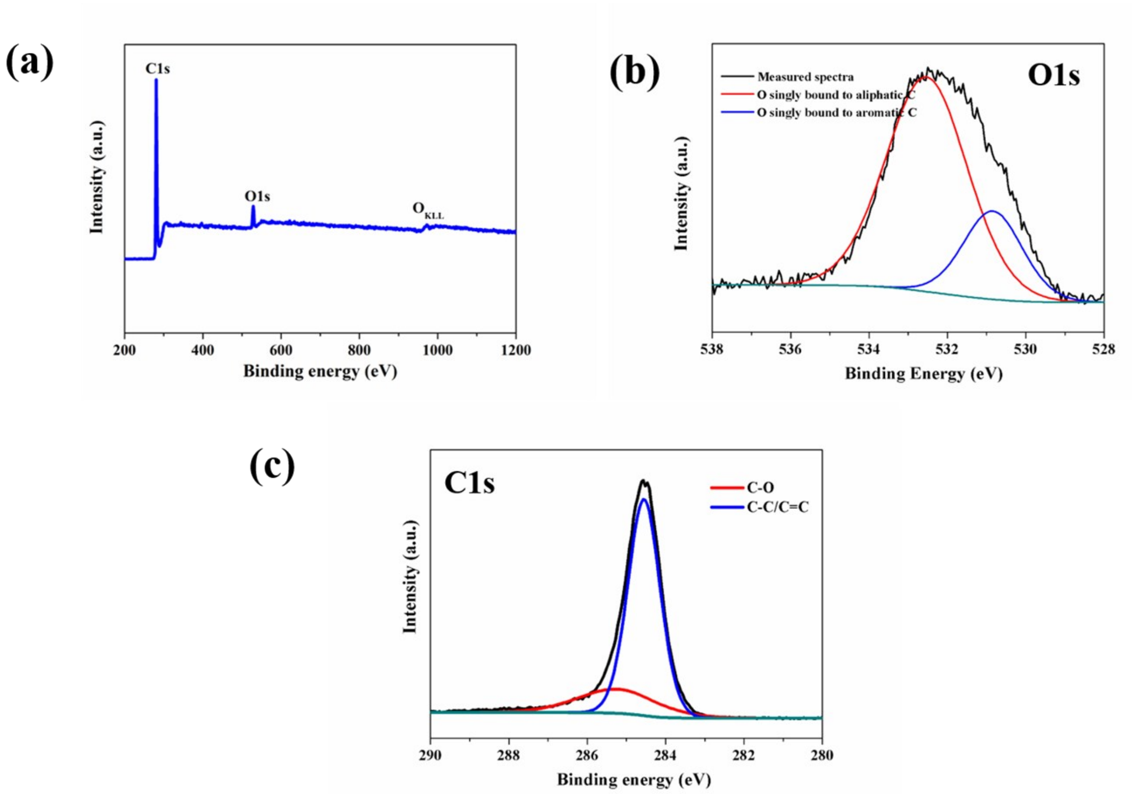

Fig. S4, XPS survey spectra of GCP-2-800 (a), deconvoluted O1s (b) and C1s spectra (c).

The XPS survey spectrum of GCP-2-800 is shown in Fig. S4. The two distinct peaks at 284.6 eV and 532.2 eV correspond to binding energies of C1s and O1s electrons, respectively. The oxygen heteroatoms contribute to pseudocapacitance, for which the charge discharge curves are not highly linear. Fig. S4b shows the deconvolution of O1s peaks, with two peaks corresponding to C-O single bond.[1] The C1s spectrum in Fig S4c was also fitted to two peaks located at 284.6 eV and 285.6 eV, corresponding to C-C/C=C and C-O, respectively.[1] Based on the above XPS analysis, the oxygen heteroatoms contributed to pseudocapacitance which may cause the charge-discharge curves are not highly linear.

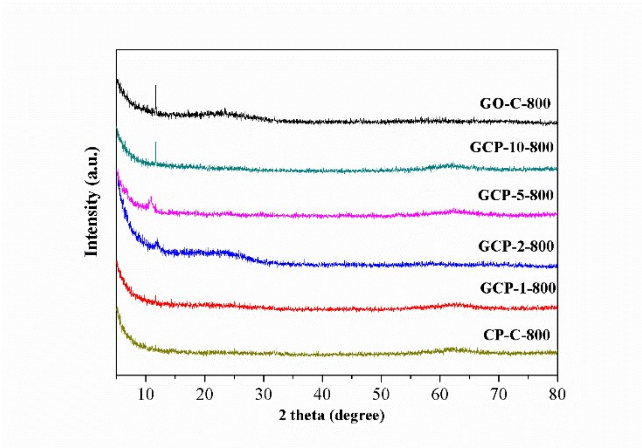

Fig. S5 XRD patterns of GO-C-800, GCP-1-800, GCP-2-800, GCP-5-800, GCP-10-800 and CP-C-800.

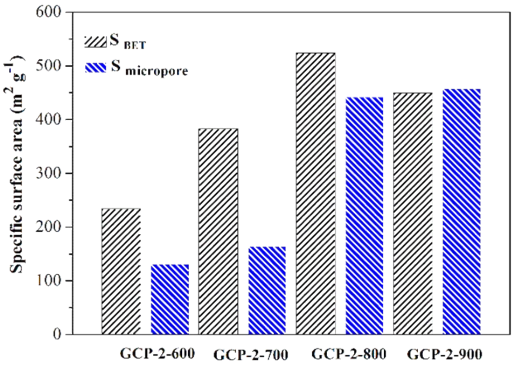

Fig. S6 SSA and micropore surface area of GCP-2-600, GCP-2-700 and GCP-2-800, GCP-2-900.

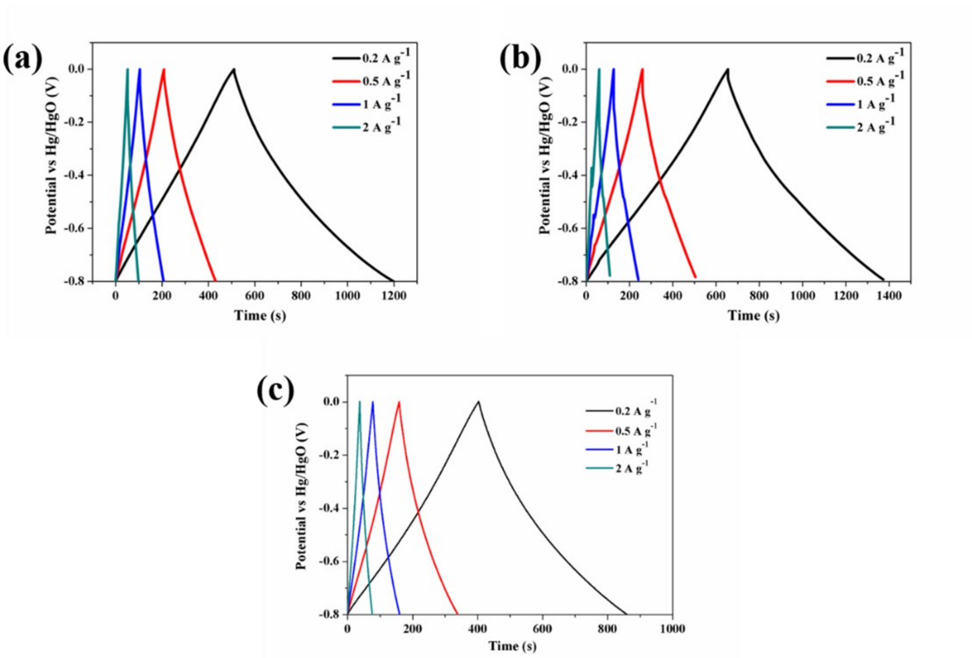

Fig. S7 GCD curves of (a) GCP-2-600 and (b) GCP-2-700 in 6 M KOH aqueous electrolyte, and (c) GCP-2-900 in 6 M KOH aqueous electrolyte.

Table S2 Comparison of the electrochemical properties of graphene-cellulose composite materials

Materials	Preparation method	Capacitance in aqueous electrolyte	Capacitance in gel electrolyte	Cycling stability %, (NO. of cycles)
RGO/CF composite (**this work**)	Impregnation + KOH activation	220 F g^{-1} at 0.2 A g^{-1}	49 mF cm^{-2} at 2 mV s^{-1} in PVA-H_2SO_4	97.6%, (10,000) at 1 A g^{-1} in aqueous electrolyte
Graphene cellulose paper membrane[2]	Vacuum filtration	120 F g^{-1} at 1 mV s^{-1} of graphene	46 mF cm^{-2} at 2 mV s^{-1} in PVA-H_2SO_4	>99%,(5,000) at 50 mV s^{-1} in aqueous electrolyte
Graphene cellulose tissue composite[3]	Vacuum filtration	60 mF cm^{-2} at 0.5 A cm^{-2}	54 mF cm^{-2} at 80 mA cm^{-2} in PVA-H_2SO_4	95%, (5,000) at 5 A g^{-1} in aqueous electrolyte
Graphite/cellulose paper[4]	Directly drawing	23 mF cm^{-2} at 0.2 A g^{-1} (23 F g^{-1})	-	>90%,(15,000) at 5 A g^{-1} in aqueous electrolyte
PANI-RGO/CP composite paper[5]	Dipping and drying +hydrothermal	464 F g^{-1} at 1 A g^{-1}	224 F g^{-1} at 0.1 A g^{-1} in PVA-H_2SO_4	89%, (1,000) at 0.1 A g^{-1} in gel electrolyte)
Bacterial cellulose paper and CNT[6]	Vacuum filtration	-	20.2 mF cm^{-2} at 1 A g^{-1} in ion gel	>99.5%, (5,000) at 10 A g^{-1} in gel electrolyte
Bacterial cellulose and graphene oxide[7]	Cross-linking	160 F at 0.4 A g^{-1}	-	90.3% (2000) at 0.4 A g^{-1} in aqueous electrolyte
Bacterial cellulose and reduced graphene oxide[8]	Bio assembly	-	65.3 F g^{-1} at 5 mV s^{-1} in PVA-H_3PO_4	88% (5000) at 1 A g^{-1} in gel electrolyte
Cellulose nanofibril and reduced graphene oxide/carbon nanotube[9]	Freeze drying +heating	-	252 F g^{-1} at 0.5 A g^{-1} in PVA-H_2SO_4	99.5% (1000) at 1 A g^{-1} in gel electrolyte

References

1. Luong, N. D.; Pahimanolis, N.; Hippi, U.; Korhonen, J. T.; Ruokolainen, J.; Johansson, L.-S.; Nam, J.-D.; Seppälä, J., Graphene/cellulose nanocomposite paper with high electrical and mechanical performances. *Journal of Materials Chemistry* **2011,** *21* (36), 13991-13998.
2. Weng, Z.; Su, Y.; Wang, D.-W.; Li, F.; Du, J.; Cheng, H.-M., Graphene–Cellulose Paper Flexible Supercapacitors. Advanced Energy Materials 2011, 1 (5), 917-922.
3. Sevilla, M.; Ferrero, G. A.; Fuertes, A. B., Graphene-cellulose tissue composites for high power supercapacitors. Energy Storage Materials 2016, 5, 33-42.
4. Zheng, G.; Hu, L.; Wu, H.; Xie, X.; Cui, Y., Paper supercapacitors by a solvent-free drawing method. Energy & Environmental Science 2011, 4 (9), 3368-3373.
5. Liu, L.; Niu, Z.; Zhang, L.; Zhou, W.; Chen, X.; Xie, S., Nanostructured Graphene Composite Papers for Highly Flexible and Foldable Supercapacitors. Advanced Materials 2014, 26 (28), 4855-4862.
6. Kang, Y. J.; Chun, S.-J.; Lee, S.-S.; Kim, B.-Y.; Kim, J. H.; Chung, H.; Lee, S.-Y.; Kim, W., All-Solid-State Flexible Supercapacitors Fabricated with Bacterial Nanocellulose Papers, Carbon Nanotubes, and Triblock-Copolymer Ion Gels. ACS Nano 2012, 6 (7), 6400-6406.
7. Liu, Y.; Zhou, J.; Zhu, E.; Tang, J.; Liu, X.; Tang, W., Facile synthesis of bacterial cellulose fibres covalently intercalated with graphene oxide by one-step cross-linking for robust supercapacitors. Journal of Materials Chemistry C 2015, 3 (5), 1011-1017.
8. Guan, F.; Chen, S.; Sheng, N.; Chen, Y.; Yao, J.; Pei, Q.; Wang, H., Mechanically robust reduced graphene oxide/bacterial cellulose film obtained via biosynthesis for flexible supercapacitor. Chemical Engineering Journal 2019, 360, 829-837.
9. Zheng, Q.; Cai, Z.; Ma, Z.; Gong, S., Cellulose Nanofibril/Reduced Graphene Oxide/Carbon Nanotube Hybrid Aerogels for Highly Flexible and All-Solid-State Supercapacitors. ACS Applied Materials & Interfaces 2015, 7 (5), 3263-3271.